JACS
JOURNAL OF THE AMERICAN CHEMICAL SOCIETY
Communication
pubs.acs.org/JACS

Surface Plasmon Mediated Chemical Solution Deposition of Gold Nanoparticles on a Nanostructured Silver Surface at Room Temperature

Jingjing Qiu,[†] Yung-Chien Wu,[†] Yi-Chung Wang,[†] Mark H. Engelhard,[‡] Lisa McElwee-White,*[,†] and Wei David Wei*[,†]

[†]Department of Chemistry and Center for Nanostructured Electronic Materials, University of Florida, Gainesville, Florida 32611, United States

[‡]Environmental Molecular Sciences Laboratory, Pacific Northwest National Laboratory, Richland, Washington 99354, United States

Supporting Information

ABSTRACT: Sub-15 nm Au nanoparticles have been fabricated on a nanostructured Ag surface at room temperature via a liquid-phase chemical deposition upon excitation of the localized surface plasmon resonance (SPR). Measurement of the SPR-mediated photothermal local heating of the substrate surface by a molecular thermometry strategy indicated the temperature to be above 230 °C, which led to an efficient decomposition of CH_3AuPPh_3 to form Au nanoparticles on the Ag surface. Particle sizes were tunable between 3 and 10 nm by adjusting the deposition time. A surface-limited growth model for Au nanoparticles on Ag is consistent with the deposition kinetics.

Nanostructures with sub-15 nm dimensions have attracted significant interest due to their unique chemical and physical properties and potential applications in catalysis,[1,2] sensing,[3] and nanofabrication for the next generation of electronic devices.[4] However, the fabrication of these nanostructures on large-scale surfaces by traditional "top-down" lithographic methods[5] remains a great challenge. The future development of these nanomaterials will rely on "bottom-up" nanoscale approaches, which allow the construction of materials from molecular or atomic components.[6,7] Utilizing the intrinsic surface properties to direct and control surface chemistry for nanostructure growth on substrate surfaces has drawn significant attention and shown the potential to greatly enhance the development of "bottom-up" approaches. For example, surface chemical bonding has been used to induce hierarchical self-assembly to form nanostructures with diverse properties.[8]

Localized surface plasmon resonance (SPR) is a unique optical property of nanoscale metallic structures (e.g., Au, Ag, Cu, and Al). In the presence of an oscillating electromagnetic field, free electrons in the conduction band of metal nanoparticles undergo a collective coherent oscillation with respect to the positive metallic lattice.[9,10] The electronic oscillation can be viewed as a photon confined to a small region of the nanostructures, constituting an intense electromagnetic (EM) field on the surface of the nanoparticles. SPR-enhanced fields are predicted to be several orders of magnitude greater than the incident optical excitation field.[11−13] They also dramatically enhance the absorption of visible light and significantly increase the yield of excited conduction electrons from their ground state to an excited state (called "hot electrons").[14] These "hot electrons" subsequently relax through nonradiative decay channels and release the excitation energy into heat, raising the temperature on localized "hot spots." Within several milliseconds, the heat dissipates between the metal lattice and the surrounding matrix (e.g., water), eventually leading to a steady-state temperature distribution.[15] Using a laser as the irradiation source, the local temperature on specific "hot spots" can be raised so as to melt or reshape nanostructures[16] and break strong chemical bonds, such as Au−S.[17] Such high temperatures can be used to promote many types of chemical reactions[18−25] on the surface of those localized "hot spots", including traditional chemical vapor deposition (CVD) reactions.[26−28] Additionally, SPR has been used for photomediated nanoparticle growth.[29−32]

Here, we report a "bottom-up" approach to fabricating sub-15 nm Au nanoparticles on a nanostructured Ag surface via a liquid-phase chemical deposition by employing localized SPR excitation. With a low power Xenon lamp, the SPR-induced surface temperature on the Ag substrate can be controlled to induce the decomposition of methyl triphenylphosphine gold (CH_3AuPPh_3), thus forming Au nanoparticles on the Ag surface in solution at room temperature. The Au surface concentration increases toward an apparent asymptote with the deposition time, indicating that the SPR-mediated deposition is a surface-limited process. Furthermore, the sizes of the Au nanoparticles can be tuned anywhere between 3 and 10 nm by adjusting the deposition time. Compared with traditional deposition methods such as CVD,[33] our approach offers mild operating conditions and low energy consumption. This surface plasmon-mediated photothermal strategy should be applicable to the controlled chemical deposition of other suitable materials.

In a typical experiment, modified nanosphere lithography[34] was used to fabricate the Ag film on nanosphere (AgFON) substrate, which consists of a hexagonally close-packed silica nanosphere (540 nm diameter) monolayer with a 150 nm thick Ag film on top, as shown in Figure S-3. The fabricated AgFON substrate shows distinctive broad SPR features in the visible region of the spectrum (Figure S-4) that are consistent with a

Received: September 21, 2012
Published: December 16, 2012

   dx.doi.org/10.1021/ja309392x | J. Am. Chem. Soc. 2013, 135, 38−41

previous report.[34] It should be noted that these unique optical properties of the AgFON substrate remain unchanged at temperatures up to 538 K.[34] Therefore, such AgFON substrates can be used to conduct high-temperature chemical reactions initiated by the SPR-mediated photothermal effect without thermal damage to the substrate.

SPR excitations on the surface of the AgFON substrate cause photothermal heating due to the nonradiative damping of SPR. In our approach, under the continuous irradiation of a Xenon lamp (power density at the sample: 2 W/cm^2), the surface temperature of the AgFON substrate is expected to rise quickly to a constant elevated value. Knowing the value of the surface temperature greatly facilitates the choice of chemical reactions for depositions. However, due to limitation on spatial resolution, conventional thermometers cannot be employed to investigate this nanoscale surface property. As an alternative, we adopted a molecular approach by using the photothermally induced polymerization of soybean oil as a local probe of the surface temperature. Soybean oil is a mixture of triglycerides that comprise three fatty acids linked by a glycerol center, and its thermal polymerization can be initiated at 230 °C in the absence of catalyst.[35] The extent of polymerization can be characterized by the decrease of the Raman peak ratio of vinyl C−H (3014 cm^{-1}) over aliphatic C−H (2855 cm^{-1}).[36] After a 3 h irradiation of the AgFON substrate in the presence of soybean oil, we observed that the Raman intensity ratio of the characteristic peaks of vinyl C−H (3014 cm^{-1}) to aliphatic C−H (2855 cm^{-1}) decreased, which indicates the initiation of the polymerization of soybean oil on the AgFON substrate (Figure S-5). Such observations demonstrate that the surface temperature reaches at least 230 °C when irradiated with 2 W/cm^2 for 3 h.

Knowledge of the surface temperature allows us to choose suitable chemical precursors for deposition of target materials. The Au precursor, CH_3AuPPh_3, was chosen because this compound decomposes between 160 and 220 °C as determined by thermogravimetric analysis (TGA) (Figure S-6). The molecule itself also shows no optical absorption in the visible region of the spectrum (Figure S-7). Since the decomposition of CH_3AuPPh_3 occurs below the threshold for the observed polymerization of soybean oil, irradiation with 2 W/cm^2 for 3 h on the AgFON substrate should create surface temperatures high enough for the decomposition of the precursor to deposit Au on Ag.

The scanning electron microscope (SEM) images show an obvious morphology change on the Ag surface after the irradiation of the AgFON substrate in the presence of a benzene solution of CH_3AuPPh_3. Specifically, a significant quantity of small nanoparticles formed on the surface of the AgFON substrate (Figure 1b). In addition to the characteristic peaks of Ag, energy dispersive X-ray spectroscopy (EDX) reveals a distinct peak at around 2.1 keV, indicating that the chemical composition of these newly formed nanoparticles is elemental Au (Figure 1c). The chemical state of the Au is further confirmed by a detailed element scan by X-ray photoelectron spectroscopy (XPS) (Figure 1d), which shows a binding energy (BE) of 84.2 ± 0.2 eV for the Au 4f$_{7/2}$. The observed BE is consistent with Au(0) in metallic Au nanoparticles.[37] Compared to the BE of Au(I) in the precursor (85.0 ± 0.2 eV), this BE downshift clearly demonstrates that the deposition of Au nanoparticles on a Ag substrate can be realized through an SPR mediated photothermal decomposition of a conventional CVD precursor through a solution phase process. It is worth noting that the bulk solution temperature was monitored via a thermocouple during the deposition process, and it was below 40 °C despite irradiation for 3 h.

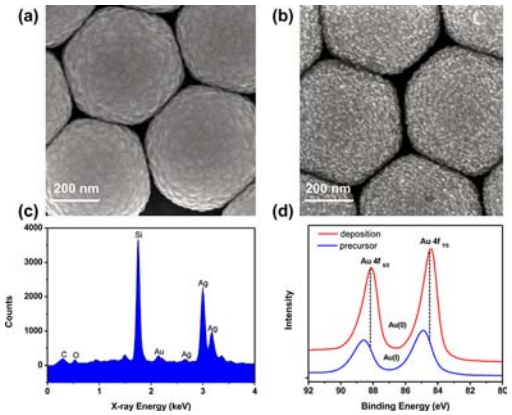

Figure 1. Au nanoparticles formed on the AgFON surface after a 3 h irradiation in a benzene solution of CH_3AuPPh_3. (a) SEM image of the AgFON substrate before deposition; (b) SEM image of the AgFON substrate after 3 h deposition; (c) Energy dispersive X-ray spectroscopy (EDX) spectrum of the AgFON substrate after the deposition of Au nanoparticles; (d) X-ray photoelectron spectroscopy (XPS) high resolution spectra of CH_3AuPPh_3 (blue) and Au nanoparticles on the AgFON substrate after the deposition (red).

The thermal decomposition mechanism of CH_3AuPPh_3 has been studied previously.[38,39] The decomposition in solution is first order in Au and the rate is decreased by the addition of free phosphine, consistent with PPh_3 dissociation as the rate-determining step. The quantitative formation of ethane in the solution decomposition of CH_3AuPPh_3 (even in the presence of good hydrogen donor solvents) rules out homolysis of the CH_3−Au bond, leaving reductive elimination of two methyl groups after Au−Au coupling as the most likely mechanism for alkyl loss and generation of metallic Au.[38,39] Our observations from XPS are consistent with this postulated mechanism. The XPS spectrum of the precursor contains a P 2p peak (BE = 131.8 ± 0.2 eV[40]) and the characteristic shake-up feature of phenyl groups (BE = 292.0 ± 0.2 eV[41]); however, neither peak is observable in the XPS spectra of the AgFON substrate after the Au deposition (Figure S-8). Such findings prove that the dissociated ligand (PPh_3) was not detectable on the surface of the AgFON substrate and suggest that the deposition of Au from the photothermal decomposition of CH_3AuPPh_3 shares common mechanistic features with conventional thermolysis. Moreover, consistent with previous reports,[38,39] ethane (CH_3CH_3) was detected in the headspace gases following the deposition (Figure S-11).

To more closely examine the photothermal decomposition of CH_3AuPPh_3 on the Ag surface, we studied the Au deposition kinetics by monitoring the change of the atomic concentration ratio of Au to Ag on the surface of the AgFON substrate over the course of the deposition. As shown in Figure 2h, in the initial stage, the Au deposition is rapid, but slows over time. This nonlinear behavior indicates that the SPR-mediated Au deposition on the AgFON substrate could be a surface-limited process. It should be noted that both the Au nanoparticle density and average particle size increase along with the deposition time (Figure 2a−g), which indicates that the surface area of Au nanoparticles should increase with time. Therefore, the photothermal decomposition of precursor molecules cannot be taking place by autocatalysis on Au nanoparticles. On the other hand, as the deposited Au nanoparticles increase, they occupy more and

dx.doi.org/10.1021/ja309392x | J. Am. Chem. Soc. 2013, 135, 38−41

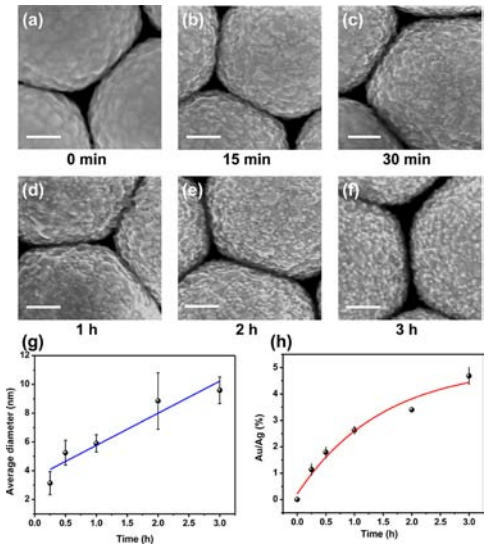

Figure 2. Au nanoparticle deposition kinetics on AgFON substrate. (a–f) SEM images of morphology change on AgFON substrate with deposition time (scale bars 100 nm); (g) increase of average Au nanoparticle size with deposition time (error bars represent the standard deviation); (h) change of Au to Ag atomic concentration ratio with deposition time (error bars represent the standard deviation).

more Ag surface area on the AgFON substrate, reducing the portion of the Ag surface area available to react with the precursor molecules during the photothermal decomposition. Alternatively, the newly formed Au nanoparticles might change the optical absorption of the AgFON substrate in such a way as to reduce the SPR-induced photothermal effect. However, an extinction spectrum of the substrate after the deposition of Au nanoparticles was indistinguishable from that of the AgFON substrate (Figure S-10). Therefore, the SPR mediated photothermal decomposition of CH_3AuPPh_3 on the AgFON substrate can be understood in terms of a mechanism modified from the one proposed for CVD of Au films from CH_3AuPPh_3 (Scheme 1):[39]

Scheme 1. Proposed Mechanism for SPR-Mediated Photothermal Decomposition of CH_3AuPPh_3 on AgFON

$$\text{Ag (surface)} + CH_3AuPPh_3 \longrightarrow CH_3Au\ \text{(Ag surface)} + PPh_3\ \text{(Ag surface)}$$

$$PPh_3\ \text{(Ag surface)} \longrightarrow \text{Ag (surface)} + PPh_3$$

$$CH_3Au\ \text{(Ag surface)} \longrightarrow \text{Au nanoparticles (Ag surface)} + \tfrac{1}{2}\ CH_3CH_3$$

The SPR excitations on the AgFON substrate raise the surface temperature high enough to activate the adsorbed precursor molecules. Subsequently, the dissociative chemisorption of CH_3AuPPh_3 produces surface methylgold fragments and PPh_3 on the Ag surface. The following decomposition of surface methylgold fragments to generate metallic Au nanoparticles could involve multiple processes, including the dinuclear reductive elimination of ethane to form Au(0),[38,39] the surface diffusion and coalescence of Au atoms, and the formation of bigger Au nanoparticles. Since small Au nanoparticles have a much higher surface energy than that of the Ag surface,[42,43] it is very likely that Au atoms (clusters) on the Ag surface tend to diffuse to and merge with nearby Au nanoparticles to form bigger Au nanoparticles in order to lower the surface energy and stabilize the Au nanoparticles. The proposed growth model is consistent with the observed linear increase of Au nanoparticle size.

Figure 2 shows the evolution of the deposited Au nanoparticles on the AgFON substrate. By controlling the deposition time, the particle sizes can be easily tuned between 3 and 10 nm, much smaller than Au nanoparticles fabricated under conventional CVD conditions.[33] Compared to the similar smaller-sized Au nanoparticles fabricated via wet chemical methods,[2] these particles are notably different in that their surfaces are free of organic ligand protection, as confirmed from the XPS measurement (Figure S-8). Additionally, it is noted that these Au nanoparticles were formed on the Ag surface at temperatures above 230 °C, and are therefore expected to be thermally stable under high temperature operating conditions.

The critical role of the Ag surface comes from the limited heat transfer from Ag to Au and the high surface energy of the created Au nanoparticles. As expected, the SPR-induced local heat is generated on the Ag surface and the heat transfer from Ag surface to Au nanoparticles is inhibited due to the low thermal conductivity of small Au nanoparticles.[44] Additionally, we have fabricated Au film on nanosphere (AuFON) and tested the photothermal polymerization of soybean oil on the Au substrate as it is known that Au nanoparticles can also absorb visible light.[15] However, under identical irradiation, we did not observe any change in the Raman intensity ratio of the characteristic peaks of vinyl C–H (3014 cm^{-1}) to aliphatic C–H (2855 cm^{-1}) (Figure S-12), consistent with that the Au thin film absorbs less of the incident light (515 to 700 nm) than the Ag thin film.[45] This observation indicates that in the process of Au nanoparticle deposition on the AgFON substrate, the newly formed Au nanoparticle surface might not reach a temperature as high as AgFON surface when irradiated with a Xenon lamp, and therefore could not cause the decomposition of CH_3AuPPh_3 on the Au nanoparticle surface.

To further demonstrate that SPR excitation of the AgFON substrate is essential to mediate the photothermal deposition of Au nanoparticles, we repeated the same experiments in the dark. As expected, no morphology change was observed on the surface of the AgFON substrate (Figure S-13a) and no Au was found via EDX measurement. In addition, we replaced the AgFON with a piece of silicon wafer. However, no deposition of Au was detected on the surface of the silicon wafer after 3 h of irradiation with the exact same power (Figure S-13b). This observation also confirms that visible light irradiation cannot cause the decomposition of the precursor molecules, consistent with the lack of visible light absorption by CH_3AuPPh_3 in the wavelength range of the light source (Figure S-7). Furthermore, we discovered that the Au nanoparticle deposition is wavelength-dependent. By using 610 and 715 nm longpass filters to partially block and prevent the SPR excitation and weaken the photothermal effect, Au deposition was found to either dramatically decrease (610 nm, Figure S-13c) compared to the deposition conducted with a 515 nm longpass filter (Figure 1 and Figure S-9) or simply not occur at all (715 nm, Figure S-13d). All the above observations reinforce the hypothesis that both AgFON substrate and a proper excitation source are critical in causing the SPR excitations that allow for an efficient photothermal deposition of Au nanoparticles onto the Ag surface.

In summary, we have successfully demonstrated that the SPR excitations of a nanostructured Ag surface can be used to assist in the deposition of Au nanoparticles at room temperature. Unlike the nanoparticles synthesized through wet chemistry meth-

dx.doi.org/10.1021/ja309392x | J. Am. Chem. Soc. 2013, 135, 38–41

ods,[46,47] these Au nanoparticles are thermally stable and their surfaces are free of organic ligand protection. The deposition kinetics reveals that the deposition of Au is surface-limited by the Ag substrate. In addition, the Au nanoparticle-AgFON substrate shows a significant improvement for the surface enhanced Raman scattering (SERS) of the adsorbed 4-aminobenzenethiol (4-ABT) (Figure S-14). Using intrinsic surface optical properties to direct and control nanostructure growth is fundamentally interesting and potentially technologically important. Traditionally, CVD of Au is limited by the thermal stability of precursors during vaporization and transport. The surface plasmon mediated chemical solution deposition (SPMCSD) method in our approach allows the deposition to be conducted in the liquid phase at room temperature, offering mild operating conditions and low-energy consumption. This SPR-mediated chemical solution deposition strategy should be extendable to the deposition of many other materials for various applications.

■ ASSOCIATED CONTENT

Supporting Information

Experimental procedures, synthesis of precursor, and additional characterization of nanoparticle depositions. This material is available free of charge via the Internet at http://pubs.acs.org.

■ AUTHOR INFORMATION

Corresponding Author

wei@chem.ufl.edu; lmwhite@chem.ufl.edu

Notes

The authors declare no competing financial interest.

■ ACKNOWLEDGMENTS

We thank the National Science Foundation for support under grant CHE-1038015, the CCI Center for Nanostructured Electronic Materials. W.D.W. acknowledges and appreciates the generous support from ORAU for the Ralph E. Powe Junior Faculty Enhancement Award, Sigma Xi for the Junior Faculty Research Award from the Florida Chapter and the University of Florida (UF) for startup assistance. The authors thank Prof. Gregory Girolami for reading the manuscript. Materials characterization was conducted at the Nanoscale Research Facility (NRF) and the Major Analytical Instrumentation Center (MAIC) at UF. A portion of the research was performed using EMSL (User proposal #40065), a national scientific user facility sponsored by the Department of Energy's Office of Biological and Environmental Research and located at Pacific Northwest National Laboratory.

■ REFERENCES

(1) Hvolbaek, B.; Janssens, T. V. W.; Clausen, B. S.; Falsig, H.; Christensen, C. H.; Norskov, J. K. *Nano Today* **2007**, *2*, 14.
(2) Jin, R. *Nanotechnol. Rev.* **2012**, *1*, 31.
(3) Rosi, N. L.; Mirkin, C. A. *Chem. Rev.* **2005**, *105*, 1547.
(4) Li, C. B.; Hasegawa, T.; Tanaka, H.; Miyazaki, H.; Odaka, S.; Tsukagoshi, K.; Aono, M. *Nanotechnology* **2010**, *21*, 495304.
(5) Liddle, J. A.; Gallatin, G. M. *Nanoscale* **2011**, *3*, 2679.
(6) Romano, F.; Sciortino, F. *Nat. Mater.* **2011**, *10*, 171.
(7) Otsubo, K.; Wakabayashi, Y.; Ohara, J.; Yamamoto, S.; Matsuzaki, H.; Okamoto, H.; Nitta, K.; Uruga, T.; Kitagawa, H. *Nat. Mater.* **2011**, *10*, 291.
(8) Seto, C.; Whitesides, G. *J. Am. Chem. Soc.* **1993**, *115*, 905.
(9) Wei, W.; Li, S. Z.; Millstone, J. E.; Banholzer, M. J.; Chen, X. D.; Xu, X. Y.; Schatz, G. C.; Mirkin, C. A. *Angew. Chem., Int. Ed.* **2009**, *48*, 4210.
(10) Morton, S. M.; Silverstein, D. W.; Jensen, L. *Chem. Rev.* **2011**, *111*, 3962.
(11) Kelly, K. L.; Coronado, E.; Zhao, L. L.; Schatz, G. C. *J. Phys. Chem. B* **2003**, *107*, 668.
(12) Wei, W.; Li, S. Z.; Qin, L. D.; Xue, C.; Millstone, J. E.; Xu, X. Y.; Schatz, G. C.; Mirkin, C. A. *Nano Lett.* **2008**, *8*, 3446.
(13) Witlicki, E. H.; Johnsen, C.; Hansen, S. W.; Silverstein, D. W.; Bottomley, V. J.; Jeppesen, J. O.; Wong, E. W.; Jensen, L.; Flood, A. H. *J. Am. Chem. Soc.* **2011**, *133*, 7288.
(14) Hartland, G. V. *Chem. Rev.* **2011**, *111*, 3858.
(15) Chen, X.; Chen, Y. T.; Yan, M.; Qiu, M. *ACS Nano* **2012**, *6*, 2550.
(16) Huang, W. Y.; Qian, W.; El-Sayed, M. A. *J. Appl. Phys.* **2005**, *98*, 114301.
(17) Jain, P. K.; Qian, W.; El-Sayed, M. A. *J. Am. Chem. Soc.* **2006**, *128*, 2426.
(18) Fasciani, C.; Alejo, C. J. B.; Grenier, M.; Netto-Ferreira, J. C.; Scaiano, J. C. *Org. Lett.* **2011**, *13*, 204.
(19) Adleman, J. R.; Boyd, D. A.; Goodwin, D. G.; Psaltis, D. *Nano Lett.* **2009**, *9*, 4417.
(20) Alessandri, I.; Ferroni, M.; Depero, L. E. *J. Phys. Chem. C* **2011**, *115*, 5174.
(21) Walker, J. M.; Gou, L. F.; Bhattacharyya, S.; Lindahl, S. E.; Zaleski, J. M. *Chem. Mater.* **2011**, *23*, 5275.
(22) Alessandri, I.; Ferroni, M.; Depero, L. E. *ChemPhysChem* **2009**, *10*, 1017.
(23) Christopher, P.; Xin, H. L.; Linic, S. *Nat. Chem.* **2011**, *3*, 467.
(24) Buchkremer, A.; Linn, M. J.; Reismann, M.; Eckert, T.; Witten, K. G.; Richtering, W.; von Plessen, G.; Simon, U. *Small* **2011**, *7*, 1397.
(25) Norman, R. S.; Stone, J. W.; Gole, A.; Murphy, C. J.; Sabo-Attwood, T. L. *Nano Lett.* **2007**, *8*, 302.
(26) Boyd, D. A.; Greengard, L.; Brongersma, M.; El-Naggar, M. Y.; Goodwin, D. G. *Nano Lett.* **2006**, *6*, 2592.
(27) Hung, W. H.; Hsu, I. K.; Bushmaker, A.; Kumar, R.; Theiss, J.; Cronin, S. B. *Nano Lett.* **2008**, *8*, 3278.
(28) Cao, L. Y.; Barsic, D. N.; Guichard, A. R.; Brongersma, M. L. *Nano Lett.* **2007**, *7*, 3523.
(29) Jin, R.; Cao, Y.; Mirkin, C. A.; Kelly, K.; Schatz, G.; Zheng, J. *Science* **2001**, *294*, 1901.
(30) Maillard, M.; Huang, P.; Brus, L. *Nano Lett.* **2003**, *3*, 1611.
(31) Zhang, J.; Langille, M. R.; Mirkin, C. A. *Nano Lett.* **2011**, *11*, 2495.
(32) Paul, A.; Kenens, B.; Hofkens, J.; Uji-i, H. *Langmuir* **2012**, *28*, 8920.
(33) Palgrave, R. G.; Parkin, I. P. *J. Am. Chem. Soc.* **2006**, *128*, 1587.
(34) Litorja, M.; Haynes, C. L.; Haes, A. J.; Jensen, T. R.; Van Duyne, R. P. *J. Phys. Chem. B* **2001**, *105*, 6907.
(35) Wang, C. H.; Erhan, S. *J. Am. Oil Chem. Soc.* **1999**, *76*, 1211.
(36) Farid Uddin Farhad, S.; Abedin, K. M.; Rafiqul Islam, M.; Talukder, A. I.; Haider, A. F. M. Y. *J. Appl. Sci.* **2009**, *9*, 5.
(37) Jung, D. H.; Kim, B. H.; Lim, Y. T.; Kim, J.; Lee, S. Y.; Jung, H. T. *Carbon* **2010**, *48*, 1070.
(38) Tamaki, A.; Kochi, J. K. *J. Organomet. Chem.* **1973**, *61*, 441.
(39) Banaszak Holl, M. M. B.; Seidler, P. F.; Kowalczyk, S. P.; Mcfeely, F. R. *Inorg. Chem.* **1994**, *33*, 510.
(40) Kumar, G.; Blackburn, J. R.; Albridge, R. G.; Moddeman, W. E.; Jones, M. M. *Inorg. Chem.* **1972**, *11*, 296.
(41) Piao, H.; Enever, M. C. N.; Adib, K.; Hrbek, J.; Barteau, M. A. *Surf. Sci.* **2004**, *571*, 139.
(42) Vitos, L.; Ruban, A. V.; Skriver, H. L.; Kollár, J. *Surf. Sci.* **1998**, *411*, 186.
(43) Lu, H. M.; Jiang, Q. *J. Phys. Chem. B* **2004**, *108*, 5617.
(44) Chen, G.; Hui, P. *Appl. Phys. Lett.* **1999**, *74*, 2942.
(45) Kulkarni, D. D.; Kim, S.; Fedorov, A. G.; Tsukruk, V. V. *Adv. Funct. Mater.* **2012**, *22*, 2129.
(46) DuChene, J. S.; Niu, W.; Abendroth, J. M.; Sun, Q.; Zhao, W.; Huo, F.; Wei, W. D. *Chem. Mater.* **2012**, DOI: 10.1021/cm3020397.
(47) Millstone, J. E.; Wei, W.; Jones, M. R.; Yoo, H.; Mirkin, C. A. *Nano Lett.* **2008**, *8*, 2526.